Approximations for Unsteady-State Diffusion and Reaction in Porous Catalyst and Their Application to Packed-Bed Reactor

Dong Hyun Kim
Dept. of Chemical Engineering, Kyungpook National University, Daegu 702-701, Korea

DOI 10.1002/aic.11554

In this study, three approximations for unsteady-state diffusion, a linear adsorption, and a first-order reaction in a catalyst particle are presented. The time-domain approximations are based on a first-, a second-, and a third-order approximation of the Laplace-domain solution of the exact partial differential equation for the catalyst. All the coefficients in the approximate equations are obtained as explicit functions of the Thiele modulus and easy to evaluate. In reactor modeling with the approximations, it is observed that the ratio of the space time in the reactor and the diffusion time in the catalyst is also an important parameter affecting the accuracy of the resulting model. A longer space time or shorter diffusion time improves the prediction of the approximate reactor model so that even the first-order approximation is found to be sufficiently accurate when the ratio is over 0.9. © 2008 American Institute of Chemical Engineers *AIChE J,* 54: 2423–2431, 2008

Keywords: LDF, approximation, intraparticle diffusion, reactor modeling, simulation

Introduction

The mass balance equations for packed-bed reactors usually consist of two parts: the mass balance for the bulk flow through the reactor and the mass balance inside the catalyst particles. For steady states, the mass balance in the catalyst can be substituted equivalently with an effectiveness factor if the factor can be readily estimated at the conditions inside the reactor. In this case, only the mass balance equations for the flowing phase including the reaction term with the effectiveness factor need to be accounted for in the reactor modeling. For unsteady states, however, such simplification is not feasible since no single parameter can equivalently represent the unsteady diffusion and reaction in the catalyst particle.

The unsteady diffusion, adsorption, and reaction in a catalyst particle is described in a partial differential equation (PDE). The PDE adds an independent variable, the space coordinate in the particle, into the reactor model. The PDE is then coupled with another PDE describing the mass balance of each component in the flowing fluid phase in the reactor. The complexity of the solution is often commensurate with the number of independent variables in the model. In this regard, it is highly desirable to have an approximation of the unsteady mass balance for the catalyst without the space variable in the particle.

Kim[1] proposed two such approximations for the unsteady diffusion, adsorption, and reaction in a catalyst particle for the first time. He solved the PDE for the particle in the time domain in the form of an infinite series and derived the approximations based on the time-domain solution in terms of the average concentration in the particle. The resulting approximations do not involve the space coordinate in the particle and are represented as ordinary differential equations (ODEs) in the form of linear driving force (LDF) formulas. The two LDF formulas differ in their approximation accuracy and have been used to simplify reactor modeling.[2,3] Later,

---

Correspondence concerning this article should be addressed to D. H. Kim at dhkim@knu.ac.kr.

Szukiewicz[4] proposed a different approximation of the LDF type with a single parameter and having an apparent similarity with the PDE for the catalyst in the terms of accumulation, rate of mass transfer, and reaction rate. It is, however, theoretically shown in this study that Szukiewicz's approximation is less accurate for its assumed form than either of Kim's two preceding approximations.

In this study, three approximations with different degrees of accuracy are developed for the unsteady diffusion, adsorption, and reaction in a catalyst particle to meet a variety of desired precisions in the reactor modeling. All the coefficients in the approximate formulas are obtained as explicit functions of the Thiele modulus, which are straightforward to evaluate, rather than the infinite series in Kim's.[1] The approximations are applied to a packed-bed reactor model to examine how each approximation affects the accuracy of the reactor model.

Theory

It is shown that the dimensionless equation for unsteady-state intraparticle diffusion, a linear adsorption, and a first-order reaction in a spherical porous catalyst is given by[1]

$$\frac{\partial c}{\partial \tau} = \frac{1}{x^2}\frac{\partial}{\partial x}\left(x^2\frac{\partial c}{\partial x}\right) - \phi^2 c \tag{1}$$

The initial concentration in the catalyst is assumed to be zero. The initial and boundary conditions are

$$c(x,0) = 0, c(1,\tau) = f(\tau), \left.\frac{\partial c}{\partial x}\right|_{x=0} = 0 \tag{2}$$

Here $f(\tau)$ is an arbitrary function of time-varying concentration at the catalyst external surface. The problem can be solved easily in the Laplace-domain.

$$\begin{aligned} q(x,s) &= \int_0^\infty e^{-s\tau}c(x,\tau)d\tau = \frac{\sinh(x\sqrt{\phi^2+s})}{x\sinh\sqrt{\phi^2+s}}F(s), \\ F(s) &= \int_0^\infty e^{-s\tau}f(\tau)d\tau. \end{aligned} \tag{3}$$

The Laplace-domain solution of the volume-average concentration is

$$Q = 3\int_0^1 q(x,s)x^2dx = 3\left(\frac{\coth\sqrt{\phi^2+s}}{\sqrt{\phi^2+s}} - \frac{1}{\phi^2+s}\right)F(s) \tag{4}$$

The transfer function is

$$G(s) = \frac{Q}{F} = 3\left(\frac{\coth\sqrt{\phi^2+s}}{\sqrt{\phi^2+s}} - \frac{1}{\phi^2+s}\right) \tag{5}$$

Table 1. Coefficients of the Series Expansion of *G*(*s*)

Coefficients

$Z = \coth\phi$

$$A_0 = 3\left(\frac{Z}{\phi} - \frac{1}{\phi^2}\right)$$

$$A_1 = -\frac{3}{2}\frac{Z^2-1}{\phi^2} - \frac{3}{2}\frac{Z}{\phi^3} + \frac{3}{\phi^4}$$

$$A_2 = \frac{3}{4}\frac{Z(Z^2-1)}{\phi^3} + \frac{9}{8}\frac{Z^2-1}{\phi^4} + \frac{9}{8}\frac{Z}{\phi^5} - \frac{3}{\phi^6}$$

$$A_3 = \frac{1-Z^2}{8\phi^4}(3Z^2-1) - \frac{3}{4}\frac{Z(Z^2-1)}{\phi^5} - \frac{15}{16}\frac{Z^2-1}{\phi^6} - \frac{15}{16}\frac{Z}{\phi^7} + \frac{3}{\phi^8}$$

Asymptotes

$\phi < 1$

$$A_0 = 1 - \frac{1}{15}\phi^2 + \frac{2}{315}\phi^4$$

$$A_1 = -\frac{1}{15} + \frac{4}{315}\phi^2 - \frac{1}{525}\phi^4$$

$$A_2 = \frac{2}{315} - \frac{1}{525}\phi^2 + \frac{4}{10395}\phi^4$$

$$A_3 = -\frac{1}{1575} + \frac{8}{31185}\phi^2 - \frac{2764}{42567525}\phi^4$$

$\phi > 3.5$

$$A_0 = \frac{3}{\phi} - \frac{3}{\phi^2}$$

$$A_1 = -\frac{3}{2\phi^3} + \frac{3}{\phi^4}$$

$$A_2 = \frac{9}{8\phi^5} - \frac{3}{\phi^6}$$

$$A_3 = -\frac{15}{16\phi^7} + \frac{3}{\phi^8}$$

Next, $G(s)$ is approximated with a rational function and the corresponding approximation in time-domain is developed. The rational function is obtained as a Pade approximant of the transfer function.[5] This method has been effective in deriving high-order approximation formulas for adsorption in a porous adsorbent.[6] For this purpose, it is necessary to expand $G(s)$ in the Taylor series as follows:

$$G(s) = A_0 + A_1 s + A_2 s^2 + A_3 s^3 + \cdots \tag{6}$$

The coefficients are functions of ϕ and listed in Table 1. For ease of computation at small and large ϕ, the asymptotes of the coefficients are also listed in the table.

Approximation I

First $G(s)$ is approximated as

$$G_1(s) = \frac{b_{10}}{a_{10}+s} \tag{7}$$

In time domain, this approximation is equivalent to

$$\frac{d\bar{c}}{d\tau} = b_{10}f - a_{10}\bar{c} = a_{10}\left(\frac{b_{10}}{a_{10}}f - \bar{c}\right) \tag{8}$$

Here $\bar{c}$ is the average concentration in the catalyst particle, defined by

$$\bar{c}(\tau) = 3\int_0^1 c(x,\tau)x^2dx \tag{9}$$

The two coefficients, a_{10} and b_{10}, can be determined by matching the coefficients of the first two terms in the series expansion of $G(s)$ and $G_1(s)$. The Taylor series of $G_1(s)$ is

$$G_1(s) = b_{10}\left(\frac{1}{a_{10}} - \frac{1}{a_{10}^2}s + \frac{1}{a_{10}^3}s^2 - + \cdots\right) \tag{10}$$

Comparison of the two series gives that $A_0 = (b_{10}/a_{10})$ and $A_1 = -(b_{10}/a_{10}^2)$ and thus

$$a_{10} = -\frac{A_0}{A_1} \quad \text{and} \quad b_{10} = -\frac{A_0^2}{A_1} \tag{11}$$

The time-domain approximation is

$$\frac{d\bar{c}}{d\tau} = -\frac{A_0}{A_1}(A_0 f - \bar{c}) \tag{12}$$

This is a first-order approximation of Eq. 1 since it is correct to the first-order in the series expansion, Eq. 10.

Approximation II

$G(s)$ is approximated by

$$G_2(s) = \frac{b_{20} + b_{21}s}{a_{20} + s} \tag{13}$$

and its series expansion is

$$G_2(s) = \frac{b_{20}}{a_{20}} + \frac{a_{20}b_{21} - b_{20}}{a_{20}^2}s + \frac{-b_{21}a_{20} + b_{20}}{a_{20}^3}s^2 - \frac{-b_{21}a_{20} + b_{20}}{a_{20}^4}s^3 + \cdots \tag{14}$$

The time-domain equation that corresponds to $G_2(s)$ is

$$\frac{d\bar{c}}{d\tau} = b_{20}f - a_{20}\bar{c} + b_{21}\frac{df}{d\tau} \tag{15}$$

Three equations are necessary to determine the three coefficients in $G_2(s)$, which are $A_0 = (b_{20}/a_{20})$, $A_1 = (a_{20}b_{21} - b_{20}/a_{20}^2)$ and $A_2 = (-a_{20}b_{21} + b_{20}/a_{20}^3)$. Solving for a_{20}, b_{20}, and b_{21}, it is obtained that

$$a_{20} = -\frac{A_1}{A_2}, \quad b_{20} = -\frac{A_0A_1}{A_2}, \quad b_{21} = A_0 - \frac{A_1^2}{A_2} \tag{16}$$

The approximation is

$$\frac{d\bar{c}}{d\tau} = -\frac{A_1}{A_2}(A_0 f - \bar{c}) + \left(1 - \frac{A_1^2}{A_0A_2}\right)A_0\frac{df}{d\tau} \tag{17}$$

This is a second-order approximation since $G_2(s)$ is correct to the s^2 term in its series expansion.

Approximation III

A high-order approximation can be obtained by

$$G_3(s) = \frac{b_{30} + b_{31}s}{a_{30} + a_{31}s + s^2} \tag{18}$$

The series expansion is

$$\begin{aligned} G_3(s) = {} & \frac{b_{30}}{a_{30}} + \frac{a_{30}b_{31} - a_{31}b_{30}}{a_{30}^2}s \\ & - \frac{a_{30}b_{30} + (a_{30}b_{31} - a_{31}b_{30})a_{31}}{a_{30}^3}s^2 \\ & + \frac{(-a_{30} + a_{31}^2)(a_{30}b_{31} - a_{31}b_{30}) + a_{30}a_{31}b_{30}}{a_{30}^4}s^3 + \cdots \end{aligned} \tag{19}$$

In the time domain, the transfer function G_3 corresponds to

$$\frac{d\bar{c}}{d\tau} = -a_{31}\bar{c} + u + b_{31}f, \qquad \frac{du}{d\tau} = -a_{30}\bar{c} + b_{30}f. \tag{20}$$

As before, the four coefficients in G_3 are determined by equating the first four terms in the expansion of Eq. 19 with the corresponding terms in $G(s)$. This gives

$$\begin{aligned} a_{30} &= \frac{A_0A_2 - A_1^2}{A_1A_3 - A_2^2}, \quad a_{31} = \frac{-A_0A_3 + A_1A_2}{A_1A_3 - A_2^2} \\ b_{30} &= A_0a_{30}, \quad b_{31} = \frac{2A_0A_1A_2 - A_0^2A_3 - A_1^3}{A_1A_3 - A_2^2} \end{aligned} \tag{21}$$

Equation 20 is a third-order approximation of Eq. 1.

When necessary, higher-order approximations, more accurate than Eq. 20, can be obtained systematically by employing more terms in the approximation of $G(s)$. It is, however, thought that the three approximations presented here are sufficient in most practical applications.

Discussion

Comparison with previous approximations

Kim[1] proposed two approximations:

$$\frac{d\bar{c}}{d\tau} = \frac{s_1}{s_2}(s_1 f - \bar{c}) \tag{22}$$

$$\frac{d\bar{c}}{d\tau} = \frac{s_2}{s_3}(s_1 f - \bar{c}) + \left(1 - \frac{s_2^2}{s_1s_3}\right)s_1\frac{df}{d\tau} \tag{23}$$

where $s_k = \sum_{n=1}^{\infty} \frac{6}{(\phi^2 + n^2\pi^2)^k}$.

According to Kim, the solution of Eqs. 1 and 2 is

$$c(x,t) = \frac{2}{x}\sum_{n=1}^{\infty}(-1)^{n+1}n\pi\,\sin(n\pi x)e^{-\lambda_n\tau}\int_0^{\tau} e^{\lambda_n\xi}f(\xi)d\xi, \qquad \lambda_n = \phi^2 + n^2\pi^2 \tag{24}$$

The average concentration is

$$\bar{c} = 3\int_0^1 c(x,\tau)x^2dx = 6\sum_{n=1}^{\infty}e^{-\lambda_n\tau}\int_0^{\tau}e^{\lambda_n\xi}f(\xi)d\xi \tag{25}$$

If $f(\xi) = \delta(\xi)$, an impulse function, the average concentration becomes

$$\bar{c}_\delta(\tau) = 6\sum_{n=1}^{\infty}e^{-\lambda_n\tau} \tag{26}$$

For the impulse, $F(s) = 1$ and thus $\bar{c}_\delta(\tau)$ is the inverse of the transfer function $G(s)$, Eq. 5. It is noted that

$$\lim_{s\to 0}\frac{d^k G(s)}{ds_k} = (-1)^k \int_0^\infty \tau^k \bar{c}_\delta(\tau)d\tau, \quad k = 1, 2, 3, \ldots$$

$$A_k = (-1)^k \sum_{n=1}^{\infty} \frac{6}{\lambda_n^{k+1}} \text{ or } \frac{(-1)^k}{6} A_k = \sum_{n=1}^{\infty} \frac{1}{(\phi^2 + n^2\pi^2)^{k+1}} \quad (27)$$

In view of the correspondence between the series and A_k, it is seen that the approximations, Eqs. 12 and 17, are identical to the approximation formulas, Eqs. 22 and 23, proposed by Kim.

Szukiewicz[4] proposed an approximation for Eq. 1 as follows:

$$\frac{d\bar{c}}{d\tau} = 3\Psi(f - \bar{c}) - \phi^2\bar{c}, \quad \Psi = \frac{\phi\coth\phi - 1}{1 - 3(\coth\phi/\phi - 1/\phi^2)} \quad (28)$$

Szukiewicz intuitively assumed this particular form to have an apparent similarity with Eq. 1 in terms of accumulation, diffusion and reaction. He obtained Ψ after some involved manipulation of the solution of Eq. 1 in the Laplace-Carson transform. Only one constant Ψ needs to be defined in the form, and this requires one condition for the coefficient. The condition can be readily obtained from the steady-state solutions of Eqs. 1 and 28. For a constant *f*, it is easy to obtain the steady-state solution of Eq. 28, which is

$$\bar{c} = \frac{3\Psi}{3\Psi + \phi^2} f \quad (29)$$

It is also straightforward to obtain the steady-state solution of Eq. 1 for a constant *f*, and the average concentration is given by

$$\bar{c} = 3\left(\frac{\coth\phi}{\phi} - \frac{1}{\phi^2}\right) f = A_0 f \quad (30)$$

A combination of Eqs. 29 and 30 results in the same Ψ in Eq. 28. It is thus obvious that the coefficient Ψ is a factor which makes the approximation have the correct steady state. This may also be examined from the transfer function of the approximation:

$$G_s(s) = \frac{3\Psi}{3\Psi + \phi^2 + s} = \frac{3\Psi}{3\Psi + \phi^2} - \frac{3\Psi}{3\Psi + \phi^2} s + \cdots$$
$$= A_0 - \frac{3\Psi}{(3\Psi + \phi^2)^2} s + \cdots \quad (31)$$

This series agrees with the series of $G(s)$ only in the constant term, showing that Szukiewicz's approximation is in fact a zero-order approximation. Consequently, Eq. 28 is bound to be less accurate than the first-order approximation Eq. 12, although both approximations are similar in form. Furthermore, it is not feasible to obtain a first-order or a high-order approximation by the method Szukiewicz employed in deriving Eq. 28.

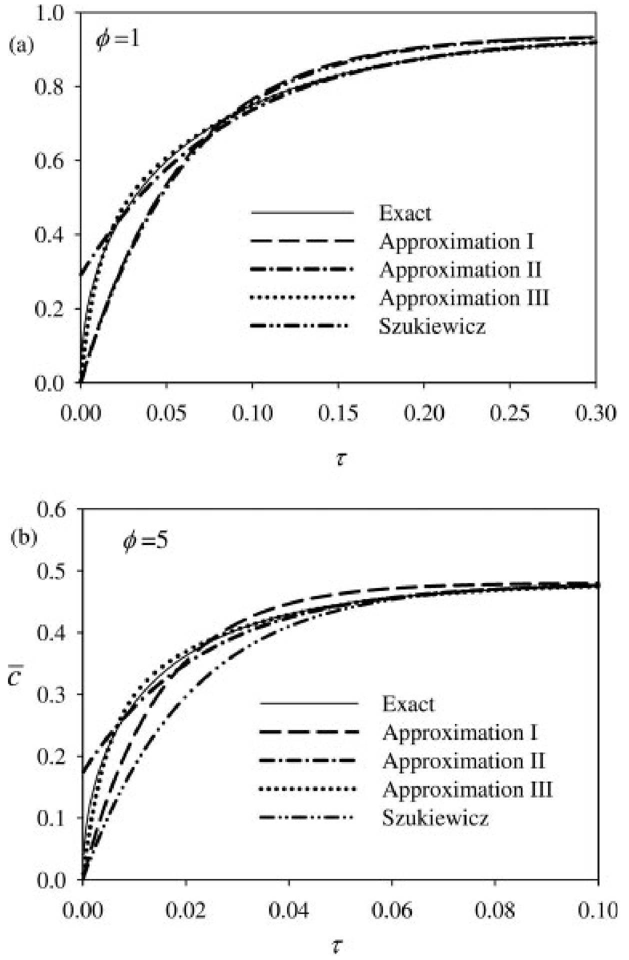

Figure 1. Comparison of the approximations for the step responses of a catalyst particle.

(a) $\phi = 1$ and (b) $\phi = 5$.

Figures 1a,b compare the approximations for a unit step change in the surface concentration, $f(\tau) = 1$ when $\tau > 0$. It is seen in the figures that the approximation accuracy increases with the increasing order of approximation. When $\phi = 1$, the step responses of Approximation I and Szukiewicz's approximation are virtually identical since, as $\phi \to 0$, both approximations become the well-known Glueckauf approximation for transient adsorption: $d\bar{c}/d\tau = 15(f - \bar{c})$.[7] On the other hand, when $\phi = 5$, the responses of the two approximations are no longer similar with each other and, in fact, Approximation I is more accurate than Szukiewicz's approximation if the accuracy is measured by

$$S_E = \int_0^\infty (\bar{c}_{\text{exact}} - \bar{c}_{\text{approx}})^2 d\tau \quad (32)$$

In Figure 1, the time to reach steady state for $\phi = 5$ is much shorter than the time for $\phi = 1$. With increasing ϕ, the concentration profile developed in the catalyst particle becomes increasingly steep and is eventually limited to the shallow skin at very large ϕ, decreasing the effective volume for diffusion and reaction in the particle and thus making the dynamics faster.

It is noted that the response of Approximation II shows a jump at $\tau = 0$. The term $df/d\tau$ in the approximation has caused such a jump because of the discontinuity at $\tau = 0$ in the applied surface concentration, a unit step function. For a continuous $f(\tau)$, the response of Approximation II would be continuous. Szukiewicz[4] commented, as a disadvantage of

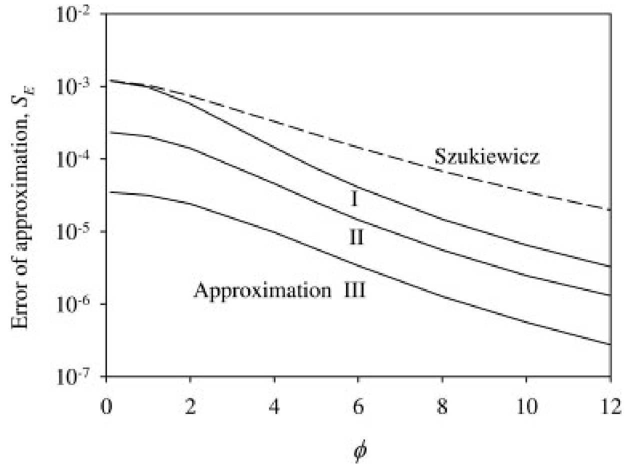

Figure 2. Comparison of errors of the approximations as calculated by Eq. 30.

Approximation II, that the surface concentration derivative $df/d\tau$ is difficult to find if the surface concentration is not given as an analytical function. This is misleading unless the dynamics of a single catalyst particle is the prime objective. The purpose of the approximations is mainly to simplify modeling of packed-bed reactors. In this case, the surface concentration is usually the concentration of the bulk fluid phase, flowing through the interstices of the bed, and its time derivative is always determined during the solution of the models. In Figure 2, the errors of the approximations as calculated by Eq. 30 are compared. It is seen that all the errors are decreasing with increasing ϕ and with the increasing order of approximation. As discussed and seen in Figure 2, Szukiewicz's approximation is least accurate among the approximations, when $\phi > 0$.

Unsteady-state packed-bed reactor

The main area for the application of the approximations is modeling unsteady-state packed-bed reactors. This study considers an isothermal, isobaric packed-bed reactor to examine the validity of the approximations in the reactor modeling. If the flow through the reactor is assumed to be plug flow with axial dispersion, the mass balance of the reactor can be given by

$$\varepsilon_b \frac{\partial C_b}{\partial t} = D_{ax}\frac{\partial^2 C_b}{\partial Z^2} - U\frac{\partial C_b}{\partial Z} - A_r D_e \frac{\partial C_p}{\partial r}\bigg|_{r=R} \tag{33}$$

Here ε_b is the catalyst bed void fraction, D_{ax} is the dispersion coefficient (m^2 s^{-1}), U is the superficial velocity (m s^{-1}), A_r is the external surface area of the catalyst particles per unit bed volume (1 m^{-1}), and D_e is the effective diffusivity in the catalyst (m^2 s^{-1}). If the catalyst particles are spheres with radius R, A_r is given by $3(1-\varepsilon_b)/R$. The mass balance in the spherical catalyst is

$$\varepsilon_p \frac{\partial C_p}{\partial t} + \frac{\partial Q}{\partial t} = \frac{D_e}{r^2}\frac{\partial}{\partial r}\left(r^2 \frac{\partial C_p}{\partial r}\right) - kC_p \tag{34}$$

ε_p is the void fraction in the catalyst particle, and Q is the adsorbed phase concentration in the catalyst and the adsorption isotherm is assumed to be linear, $Q = KC_p$. The initial and boundary conditions are

$$\begin{aligned} &C_b(Z,0) = 0,\ C_p(Z,\mathrm{r},0) = 0 \\ &C_p(Z,R,t) = C_b(Z,t), \quad \frac{\partial C_p}{\partial r}\bigg|_{\mathrm{r}=0} = 0, \\ &UC_b(0,t) - D_{ax}\frac{\partial C_b}{\partial Z}\bigg|_{Z=0} = UF_0(t), \quad \frac{\partial C_b}{\partial Z}\bigg|_{Z=L} = 0 \end{aligned} \tag{35}$$

$F_0(t)$ is a time-varying feed concentration. We define dimensionless variables and parameters.

$$\begin{aligned} &y_b = \frac{C_b}{C_0},\ y_p = \frac{C_p}{C_0},\ z = \frac{Z}{L},\ x = \frac{r}{R},\ \theta = \frac{t}{\theta_0} \\ &\theta_0 = \frac{\varepsilon_b L}{U},\ \alpha = \frac{\theta_0}{(R^2/D_e)},\ Pe = \frac{UL}{D_{ax}} \end{aligned} \tag{36}$$

The dimensionless mass balance equations are

$$\frac{\partial y_b}{\partial \theta} = \frac{1}{Pe}\frac{\partial^2 y_b}{\partial z^2} - \frac{\partial y_b}{\partial_z} - 3\frac{(1-\varepsilon_b)}{\varepsilon_b}\alpha\frac{\partial y_b}{\partial x}\bigg|_{x=1} \tag{37}$$

$$\frac{(\varepsilon_p + K)}{\alpha}\frac{\partial y_p}{\partial \theta} = \frac{1}{x^2}\frac{\partial}{\partial x}\left(x^2\frac{\partial y_p}{\partial x}\right) - \phi^2 y_p \tag{38}$$

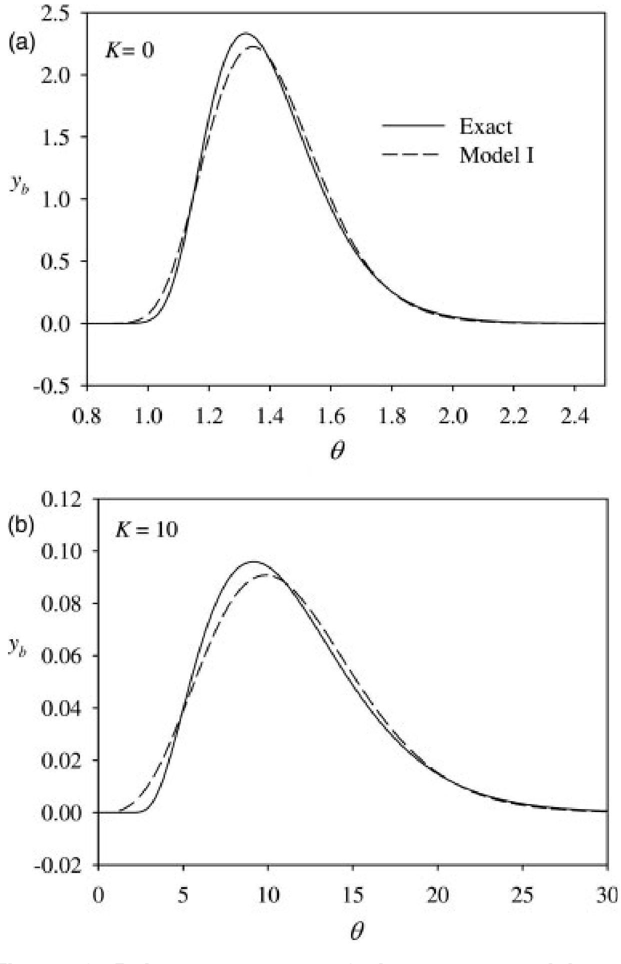

Figure 3. Pulse responses of the exact model and Model I.

Pe = 1000, α = 0.7, ε_b = 0.5, ε_p = 0.4, ϕ = 0. (a) K = 0 and (b) K = 10.

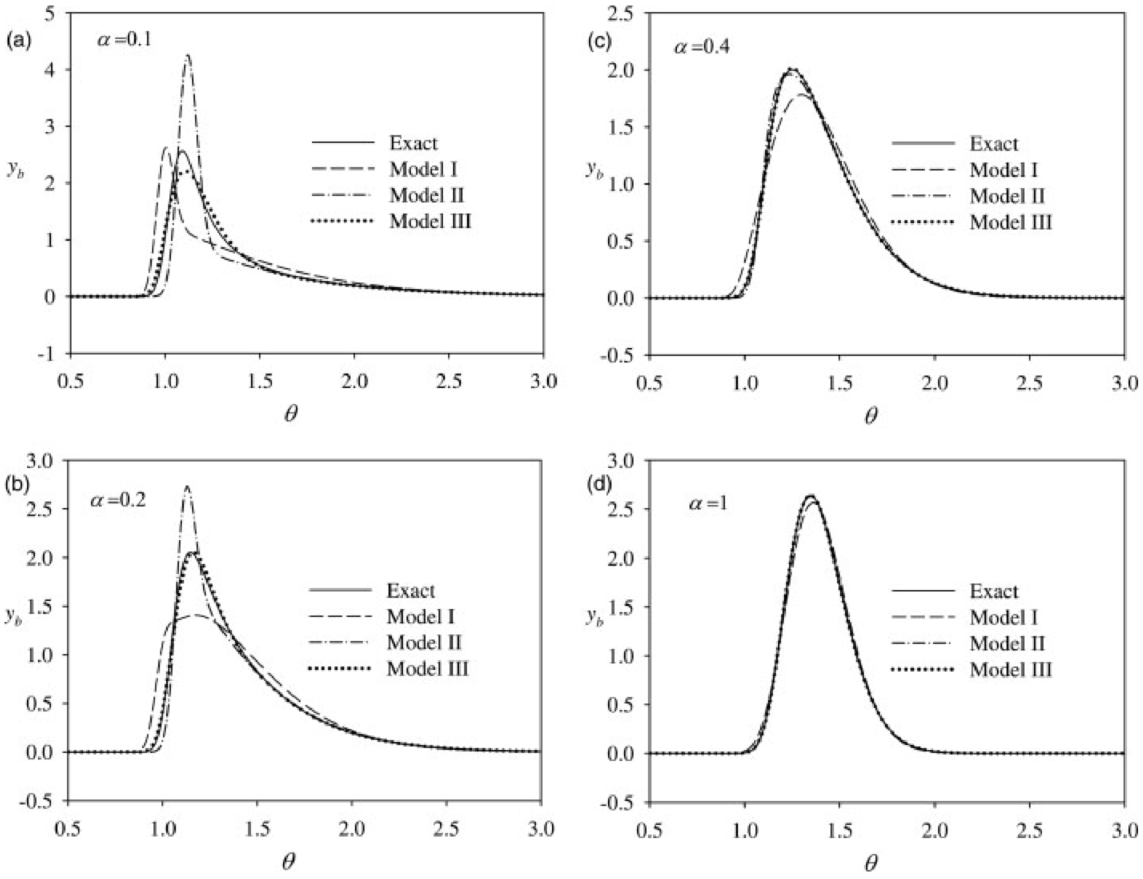

Figure 4. Effect of α on the accuracy of pulse responses of the approximate models.

Pe = 1000, K = 0, α = 0.7, ε_b = 0.5, ε_p = 0.4, ϕ = 0. (a) α = 0.1, and (b) α = 0.2, (c) α = 0.4, and (d) α = 1.

The associated conditions are

$$\begin{aligned} &y_b(z,0)=0,\ y_p(z,x,0)=0 \\ &y_p(z,1,\theta)=y_b(z,\theta),\quad \left.\frac{\partial y_p}{\partial x}\right|_{x=0}=0, \\ &y_b(0,\theta)-\frac{1}{Pe}\left.\frac{\partial y_b}{\partial z}\right|_{z=0}=f_0(\theta),\quad \left.\frac{\partial y_b}{\partial z}\right|_{z=1}=0 \end{aligned} \tag{39}$$

Integration of Eq. 38 gives

$$\begin{aligned} \left.\frac{\partial y_p}{\partial x}\right|_{x=1} &= \int_0^1 \left[\frac{(\varepsilon_p+K)}{\alpha}\frac{\partial y_p}{\partial \theta}+\phi^2 y_p\right]x^2 dx \\ &= \frac{1}{3}\left[\frac{(\varepsilon_p+K)}{\alpha}\frac{\partial \bar{y}_p}{\partial \theta}+\phi^2 \bar{y}_p\right]=\frac{1}{3}\left(\frac{\partial \bar{y}_p}{\partial \tau}+\phi^2\bar{y}_p\right) \end{aligned} \tag{40}$$

For $\partial\bar{y}_p/\partial\tau$, one of the approximations can be used. Using Approximation I, II, and III results in three approximate models, Model I, Model II, and Model III.Model I:

$$\frac{\partial y_b}{\partial \theta}=\frac{1}{Pe}\frac{\partial^2 y_b}{\partial z^2}-\frac{\partial y_b}{\partial z}-\frac{(1-\varepsilon_b)}{\varepsilon_b}\alpha\left(-\frac{A_0}{A_1}(A_0 y_b-\bar{y}_p)+\phi^2\bar{y}_p\right) \tag{41}$$

$$\frac{(\varepsilon_p+K)}{\alpha}\frac{\partial \bar{y}_p}{\partial \theta}=-\frac{A_0}{A_1}(A_0 y_b-\bar{y}_p) \tag{42}$$

Model II:

$$\begin{aligned} &\left(1+\frac{3(1-\varepsilon_b)}{\varepsilon_b}b_{21}(\varepsilon_p+K)\right)\frac{\partial y_b}{\partial \theta} \\ &\quad =\frac{1}{Pe}\frac{\partial^2 y_b}{\partial z^2}-\frac{\partial y_b}{\partial z}-\frac{(1-\varepsilon_b)}{\varepsilon_b}\alpha(b_{20}y_b-a_{20}\bar{y}_p+\phi^2\bar{y}_p) \end{aligned} \tag{43}$$

$$\frac{(\varepsilon_p+K)}{\alpha}\frac{\partial \bar{y}_p}{\partial \theta}=-a_{20}\bar{y}_p+b_{20}y_b+b_{21}\frac{(\varepsilon_p+K)}{\alpha}\frac{\partial y_b}{\partial \theta} \tag{44}$$

Model III:

$$\frac{\partial y_b}{\partial \theta}=\frac{1}{Pe}\frac{\partial^2 y_b}{\partial z^2}-\frac{\partial y_b}{\partial z}-\frac{(1-\varepsilon_b)}{\varepsilon_b}\alpha(-a_{31}\bar{y}_p+u+b_{31}y_b+\phi^2\bar{y}_p) \tag{45}$$

$$\frac{(\varepsilon_p+K)}{\alpha}\frac{\partial \bar{y}_p}{\partial \theta}=-a_{31}\bar{y}_p+u+b_{31}y_b \tag{46}$$

$$\frac{(\varepsilon_p+K)}{\alpha}\frac{\partial u}{\partial \theta}=-a_{30}\bar{y}_p+b_{30}y_b \tag{47}$$

The solutions of the exact model and the approximate models are compared. Since the models are linear, the analytic solution of each model can be easily obtained in the Laplace domain. The Laplace-domain solutions of the models are listed in the Appendix. The corresponding time-domain solutions can be easily obtained by inverting the Laplace-domain solutions numerically. The inversion method proposed by Kim and Chang[8] was used in this study. For an approximate model, its approximation accuracy was found to be mainly affected by ϕ and α, the ratio of space time (θ_0) and diffusion time (R^2/D_e). Small values of α mean short bed lengths, fast flow rates or large diffusion times. Figures 3a,b compare the pulse responses of the exact model and Model I for $\alpha = 0.7$, $\phi = 0$, and $K = 0$ or 10. Although the duration and height of the peak depend on K, the agreement between the exact model and Model I is similar for both values of K, indicating a minor effect of K on the approximation accuracy.

Figures 4a–d show the pulse responses of the models for $\phi = 0$ and various values of α. The accuracy of the approximate models improves with an increasing α. For $\alpha = 0.1$, all the models show poor accuracy, but for $\alpha = 0.2$, Model III becomes as good as the exact model, while Models I and II are still poor. A further increase in α to 0.4 makes Model II almost indistinguishable with the exact model, and at $\alpha = 1$, even Model I shows an excellent agreement with the exact model. Figures 5a,b compare the pulse responses of the models for $\alpha = 0.1$ and $\phi = 5$ and 10, showing that the accuracy of the models increases with an increasing ϕ. It is seen that Model III shows a poor accuracy when $\phi = 0$ (Figure 4a) but a satisfactory accuracy at $\phi = 5$ (Figure 5a). At $\phi = 10$, Model II shows an excellent agreement with the exact model (Figure 5b). From these figures, it is shown that the applicability of the approximations is shown to strongly depend on the values of α and ϕ.

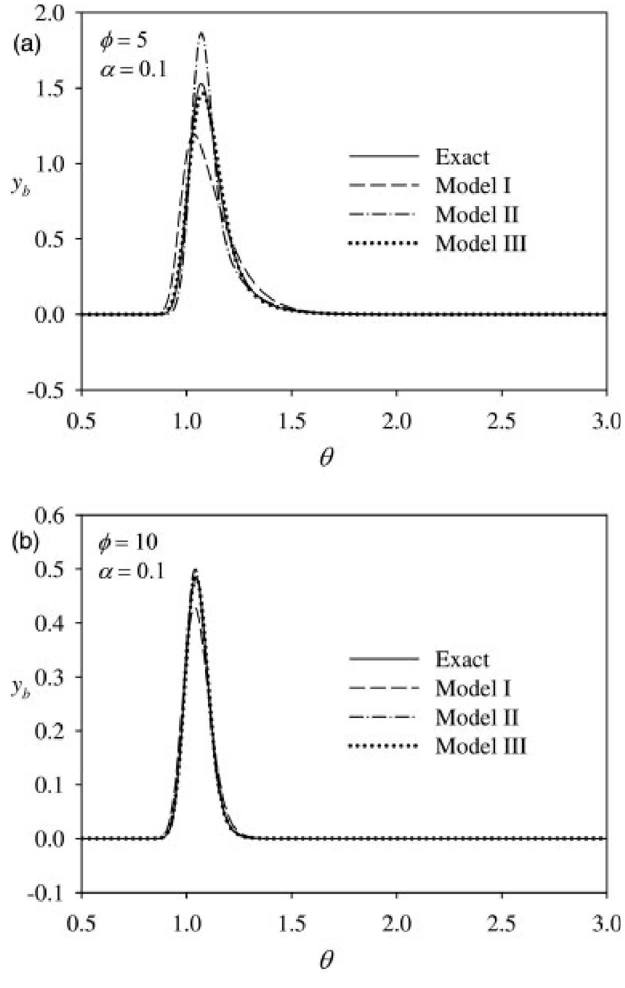

Figure 5. Effect of α on the accuracy of pulse responses of the approximate models.

$Pe = 1000$, $K = 0$, $\alpha = 0.1$, $\varepsilon_b = 0.5$, $\varepsilon_p = 0.4$. (a) $\phi = 5$ and (b) $\phi = 10$.

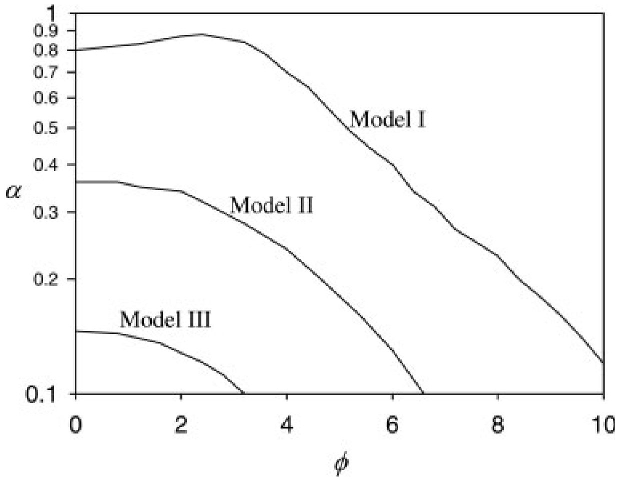

Figure 6. Lower bounds of α and ϕ for the approximations in reactor modeling.

For each approximate model, the bound for values of α and ϕ, which yielded errors less than 10% of the peak height, was computed. The three lower bounds for Models I, II, and III are shown in Figure 6. For each model, if the values of α and ϕ are larger than the values of its lower bound, the approximate model can be used instead of the exact model. When two or three models are applicable, the simpler model would be preferred unless a high precision is required. The lower bounds would indicate the valid regions for the approximations in reactor modeling. A criterion for any ϕ may be made based on Figure 6 for application of the three approximations: Approximation I when $\alpha > 0.9$, Approximation II, $\alpha > 0.35$, and Approximation III, $\alpha > 0.15$.

If the reactor model of interest is linear as in this study, the approximations may be unnecessary since the Laplace-domain solution of the exact model is easy to obtain and can be readily inverted numerically. If the bed is nonisothermal and/or a significant pressure drop is occurring along the bed, the mass balance of the bed becomes nonlinear and has to be solved numerically from the start. The reactor model involves two space variables, z for the axial position along the bed and x for the radial position in catalyst particles. If one of the approximations of this study is employed, the radial variable x disappears in the resulting model and this would considerably simplify the numerical solution.

Conclusion

Three approximations for unsteady state diffusion, a linear adsorption, and a first-order reaction in a catalyst particle are presented. First, the transfer function of an exact model for the catalyst was obtained in the Laplace domain and then approximated by rational functions, which are exact to the first-, the second-, or the third-order term in their Taylor series. The time-domain equations corresponding to the rational functions in the Laplace domain were obtained as the approximations. This method can be easily extended to obtain any other high-order approximations. In addition to the approximation order, the accuracy in the calculated results by the approximations also increased with the increasing Thiele modulus.

In reactor modeling with the approximations, the accuracy of the approximate reactor models also showed a marked dependency on the parameter α, the ratio of the space time in the reactor and the diffusion time in the catalyst. The accuracy of the model predictions improved with an increasing α, but for very low values of α the approximate reactor models failed. Numerical studies with the models yielded a range of α for each approximation: $\alpha > 0.15$ for the third-order approximation, $\alpha > 0.35$ for the second-order approximation, and $\alpha > 0.9$ for the first-order approximation.

Acknowledgments

The financial support of the Fuel-Cell Core-Technology Research Center at Korean Institute of Energy Research is gratefully acknowledged.

Notation

A_i = i-th order coefficient in the series expansion of $G(s)$
a_{ij} = j-th order coefficient in the denominator of i-th order approximation $G_i(s)$
b_{ij} = j-th order coefficient in the numerator of i-th order approximation $G_i(s)$
C_b = concentration in the fluid phase flowing through reactor (mol m^{-3})
C_p = concentration in catalyst (mol m^{-3})
$\bar{c}$ = average concentration in catalyst, dimensionless
D_ax = axial dispersion coefficient (m s^{-2})
D_e = effective diffusivity in catalyst (m s^{-2})
f = concentration at the outer surface of catalyst, dimensionless
f_0 = feed concentration, dimensionless
F = Laplace transform of f
F_0 = feed concentration (mol m^{-3})
$G(s)$ = transfer function of catalyst, defined in Eq. 5
G_1, G_2, G_3 = transfer function of first-order, second-order, and third-order approximation, respectively
K = adsorption equilibrium constant, dimensionless
k = reaction rate constant (s^{-1})
L = reactor length (m)
Pe = Peclet number, dimensionless
Q = concentration of adsorbed phase in catalyst (mol m^{-3})
R = radius of catalyst particle (m)
r = radial position in catalyst (m)
s = Laplace-domain variable
t = time (s)
U = superficial velocity in reactor (m s^{-1})
x = radial position in catalyst, dimensionless
y_b = concentration in the bulk flow, dimensionless
y_p = concentration in catalyst, dimensionless
$\bar{y}_p$ = average concentration in catalyst, dimensionless
Z = axial position in reactor (m)
z = axial position in reactor, dimensionless ($= Z/L$)

Greek letters

α = ratio of space time and diffusion time $(= \theta_0/(R^2/D_\mathrm{e}))$
ϕ = Thiele modulus $(= R\sqrt{k/D_\mathrm{e}})$
θ = time, dimensionless $(= t/\theta_0)$
θ_0 = space time, s $(= \varepsilon_\mathrm{b}L/U)$
τ = time, dimensionless $(= tD_\mathrm{e}/(R^2(\varepsilon_\mathrm{p} + K))$

Literature Cited

1. Kim DH. Linear driving force formulas for diffusion and reaction in porous catalysts. *AIChE J*. 1989;35:343–346.
2. Bidabehere CM, Sedran U. Use of stirred batch reactors for the assessment of adsorption constants in porous solid catalysts with simultaneous diffusion and reaction. Theoretical analysis. *Chem Eng Sci*. 2006;61:2048–2055.
3. Sa Gomes P, Leao CP, Rodrigues AE. Simulation of true moving bed adsorptive reactor: detailed particle model and linear driving force approximations. *Chem Eng Sci*. 2007;62:1026–1041.
4. Szukiewicz MK. New approximate model for diffusion and reaction in a porous catalyst. *AIChE J*. 2000;46:661–665.
5. Bender CM, Orszag SA. *Advanced Mathematical Methods for Scientists and Engineers*. New York: McGraw-Hill, 1978:383–389.
6. Lee J, Kim DH. High-order approximations for noncyclic and cyclic adsorption in a particle. *Chem Eng Sci*. 1998;53:1209–1221.
7. Glueckauf E. Theory of chromatography, Part 10: Formulae for diffusion into spheres and their application to chromatography. *Trans Faraday Soc*. 1955;51:1540–1551.
8. Kim DH, Chang KS. A method of numerical solution for unsteady state problems: inversion of Laplace transforms by recursive orthogonal polynomial regression. *Chem Eng J*. 1984;29:11–18.

Appendix

The Laplace domain solution of the model is

$$Y_{\mathrm{b}}(1,\mathrm{s}) = \frac{2bPeL(f_0)}{\exp(-a+b)[Pe(a+b)-(a^2-b^2)] - \exp(-a-b)[Pe(a-b)-(a^2-b^2)]} \tag{A1}$$

where $a = (Pe/2), b = (Pe/2)\sqrt{1+(4\gamma/Pe)}$, $L(f_0)$ is the Laplace transform of the feed function $f_0(\theta)$ and γ is different for the exact model and Models I, II, and III, as given in the following.

Exact model

$$\gamma = s + \frac{3(1-\varepsilon_{\mathrm{b}})}{\varepsilon_{\mathrm{b}}}\alpha\left(\sqrt{\phi^2 + s\frac{(\varepsilon_{\mathrm{p}}+K)}{\alpha}}\coth\sqrt{\phi^2 + s\frac{(\varepsilon_{\mathrm{p}}+\mathrm{K})}{\alpha}} - 1\right) \tag{A2}$$

Model I

$$\gamma = s + \frac{3(1-\varepsilon_{\mathrm{b}})}{\varepsilon_{\mathrm{b}}}\alpha\left(\left(\phi^2 + s\frac{(\varepsilon_{\mathrm{p}}+K)}{\alpha}\right)\frac{(-A_0^2/A_1)}{\left(-\frac{A_0}{A_1} + \frac{\varepsilon_{\mathrm{p}}+K}{\alpha}s\right)}\right) \tag{A3}$$

Model II

$$\gamma = s\left(1 + \frac{1-\varepsilon_{\mathrm{b}}}{\varepsilon_{\mathrm{b}}}b_{21}(\varepsilon_{\mathrm{p}}+K)\right) + \alpha\frac{1-\varepsilon_{\mathrm{B}}}{\varepsilon_{\mathrm{B}}}(b_{20} + (\phi^2 - a_{20})\Gamma)$$

$$\Gamma = \frac{b_{20} + b_{21}s(\varepsilon_{\mathrm{p}}+\mathrm{K})/\alpha}{a_{20} + s(\varepsilon_{\mathrm{p}}+\mathrm{K})/\alpha} \tag{A4}$$

Model III

$$\gamma = \mathrm{s} + \frac{3(1-\varepsilon_{\mathrm{b}})}{\varepsilon_{\mathrm{b}}}\alpha\xi$$

$$\xi = \left(\frac{b_{30}}{s(\varepsilon_{\mathrm{p}}+\mathrm{K})/\alpha} + b_{31}\right)\left(1 + \frac{\phi^2 - a_{31} - \frac{a_{30}}{s(\varepsilon_{\mathrm{p}}+\mathrm{K})/\alpha}}{s(\varepsilon_{\mathrm{p}}+\mathrm{K})/\alpha + a_{31} + \frac{a_{30}}{s(\varepsilon_{\mathrm{p}}+\mathrm{K})/\alpha}}\right) \tag{A5}$$

Manuscript received Nov. 15, 2007, revision received Mar. 15, 2008, and final revision received May 13, 2008